Available online at www.sciencedirect.com
SCIENCE DIRECT
Journal of Photochemistry and Photobiology A: Chemistry 178 (2006) 201–207
Journal of Photochemistry and Photobiology A:Chemistry
www.elsevier.com/locate/jphotochem

Solvent-assisted intramolecular vibrational energy redistribution of S_1 perylene in ketone solvents

Takayuki Kiba, Shin-ichiro Sato *, Seiji Akimoto, Tatsuya Kasajima, Iwao Yamazaki

Division of Biochemistry and Macromolecular Chemistry, Graduate School of Engineering, Hokkaido University, Sapporo 060-8628, Japan

Available online 19 December 2005

Abstract

We investigated vibrational energy relaxations of S_1 perylene at an excess energy of ca. 2800 cm^{-1} in several ketone solvents by femtosecond time-resolved fluorescence measurements. Temporal evolution of fluorescence emissions occurs on the following distinct timescales: 70–330 fs, 0.6–1.1 ps and 1.8–4.9 ps. The latter two was assigned to the intramolecular vibrational redistribution (IVR), and to the solvent-assisted IVR (SA-IVR), respectively. In SA-IVR, intramolecular vibrational couplings are affected by elastic or quasi–elastic interactions between solute and solvents. Solvent dependence of the SA-IVR rates can be explained qualitatively by the tier V–V coupling mechanism.

Keywords: Vibrational relaxation; Intramolecular vibrational energy redistribution; Intermolecular vibrational energy transfer; Fluoresence up-conversion method; Solute–solvent interaction

1. Introduction

Flow of excess vibrational energy of molecules and solvation dynamics are closely related to each other, and play important roles in various photochemical reactions in condensed phases [1,2]. Understanding of vibrational energy relaxation (VER) is prerequisite to the quantum control of photochemical reactions in condensed phases since VER disturbs quantum phases of molecules. Many experimental and theoretical studies have been reported on VER in the last decade [3–22]. Vibrational energy relaxation contains both intra- and intermolecular processes. The intramolecular process is called intramolecular vibrational redistribution (IVR), in which a vibrational excess energy initially deposited on Franck–Condon active state(s) is distributed over the other dark states within the molecule. The intermolecular processes are usually called vibrational cooling (VC) or vibrational energy transfer (VET), in which the vibrational excess energy dissipates from solute to solvent molecules by inelastic solute–solvent collisions. Recent studies have shown that IVR is further classified into two processes in solutions; the fast IVR that takes place in tens of femtoseconds to sub picoseconds time scales and the slow IVR in a few picoseconds time scale [5–8]. The slow IVR is sometimes called solvent-assisted IVR (SA-IVR), since it would be affected by elastic or quasi–elastic solute–solvent interactions [6]. However, the definition of the SA-IVR is ambiguous, and often cannot be distinguished from that of VET.

Baskin et al. studied free-base tetraphenylporphirin (H_2TPP) in benzene by using a fluorescence up-conversion and a pump-probe transient absorption spectroscopy with sub picoseconds resolution [6]. They found three relaxation times: 100–200 fs, 1.4 ps and 10–20 ps. The fastest component of 100–200 fs was assigned to IVR in the Q_x state and the slowest component of 10–20 ps was assigned to VET. The middle component of 1.4 ps was interpreted as vibrational energy redistribution caused by elastic or quasi–elastic collisions with solvent molecules. This process would be attributed to SA-IVR. von Benten et al. have examined VER of S_0 benzene and S_0 toluene in gas phase, solution, and CO_2-supercritical fluid by means of ultrafast transient absorption spectroscopy [7,8]. They found two IVR processes, and only the slower IVR was accelerated in solution and showed solvent density dependence in CO_2-supercritical fluid. These results indicated that solute–solvent interactions accelerate the IVR rate; therefore the slower IVR component can be attributed to the SA-IVR.

Blanchard et al. studied VER of S_0 perylene and S_0 1-methylperylene in various solvents by using picosecond stimulated emission spectroscopy [9–11]. They investigated VET taking place in time scales slower than tens of picoseconds. They found that VET rates of 10–50 ps in ketones and alde-

* Corresponding author. Fax: +81 11 709 2037.
E-mail address: s-sato@eng.hokudai.ac.jp (S.-i. Sato).

1010-6030/$ – see front matter © 2005 Elsevier B.V. All rights reserved.
doi:10.1016/j.jphotochem.2005.09.032

hydes are faster than those of 100–300 ps in other solvents like normal alkanes. They explained that VET acceleration is caused by strong solute–solvent interactions.

We have recently reported on VER of the vibrational excess energy of ca. 2800 cm^{-1} of S_1 perylene and S_1 12-(3-perylenyl)dodecanoic acid (PD) in 2-methyltetrahydrofuran (MTHF) with a femtosecond fluorescence up-conversion method [12,13]. The VER rate of PD is faster than that of perylene; therefore we concluded that the observed VER process includes the contribution from IVR, because the IVR rate is generally accelerated by the increase of the density of vibrational states of molecule. In the present study, we performed time-resolved fluorescence measurements on perylene in several ketone solvents in order to investigate whether this slow IVR has pure IVR or SA-IVR character.

2. Experimental section

Perylene was purchased from Sigma Chemical Company, and used without further purification. All ketone solvents (3-pentanone, 3-heptanone, 3-octanone, 3-nonanone and 3-decanone) were purchased from Aldrich in their highest purity grade and used without further purification except 3-nonanone. 3-Nonanone was used after distillation. Steady-state absorption and fluorescence spectra were measured with a spectrometer (U-3010, Hitachi) and a fluorescence spectrometer (F-4500, Hitachi), respectively. Concentrations of sample solutions were ca. 10^{-5} M for the steady-state absorption measurements while ca. 10^{-6} M for the steady-state fluorescence measurements.

Fluorescence time profiles were measured with a femtosecond fluorescence up-conversion system using a Ti: Sapphire laser (Tsunami, Spectra-Physics), pumped with a diode-pumped solid-state laser (Millennia Xs, Spectra-Physics) [23]. To avoid polarization effects, the angle between polarizations of an excitation beam and a probe beam was set to the magic angle by a λ/2 plate. The fluorescence time profiles were measured at four wavelengths according to the vibrational progression (0–0, 0–1, 0–2 and 0–3 transitions) as shown in Fig. 1. Concentrations of perylene solutions used for time-resolved fluorescence measurements were ca. 10^{-5} M.

All experiments were carried out at room temperature. Each decay curve was individually fitted to a multi-exponential function by using an iterative deconvolution method. In this analysis, a Gaussian function fitted to the up-conversion signal from a solvent, Raman scattering was used as an instrumental response function (ca. 200 fs FWHM).

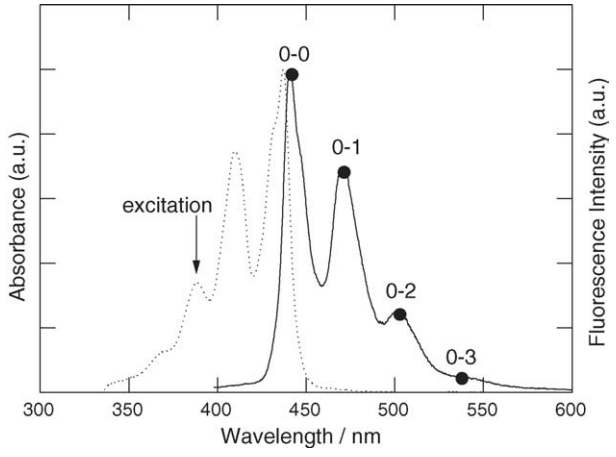

Fig. 1. Steady-state absorption (dotted line) and fluorescence (solid line) spectra of perylene in 3-octanone. An arrow indicates the excitation wavelength.

3. Results and discussion

Steady-state absorption and fluorescence spectra of perylene in 3-octanone are shown in Fig. 1. The excitation wavelength was 388 nm, which corresponds to an excitation at the 0–2 $S_1 \leftarrow S_0$ absorption band. Essentially the absorption and fluorescence spectra did not show major solvent dependence except only minor solvent-dependent band shifts.

In Figs. 2–6, the temporal profiles of fluorescence in 3-pentanone, 3-heptanone, 3-octanone, 3-nonanone and 3-decanone are displayed for 0–0, 0–1, 0–2 and 0–3 vibrational transitions following the excitation at the 0–2 $S_1 \leftarrow S_0$ absorption band, respectively. The distinguished wavelength dependence of the fluorescence rise-and-decay curves within the same electronic transition is consistent with characteristics of VER [12,13].

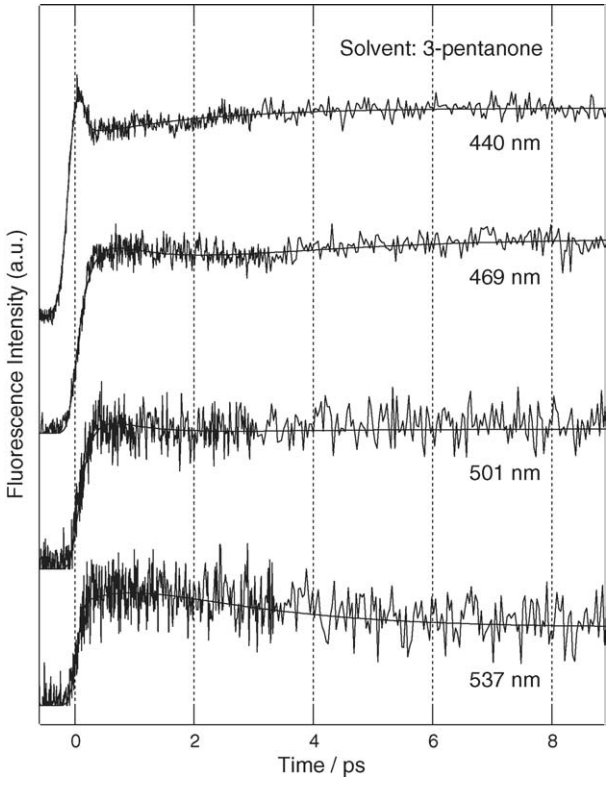

Fig. 2. Fluorescence time profiles measured with a femtosecond fluorescence up-conversion method for perylene in 3-pentanone. Observed wavelengths are indicated in the figure. Each fluorescence transients was deconvoluted with an instrumental response function of 200 fs FWHM, and then fitted to a sum of exponential terms, $\sum A_i \exp(-t/\tau_i)$, with independent amplitude, A_i, and lifetime, τ_i. Solid lines are fits of experimental data.

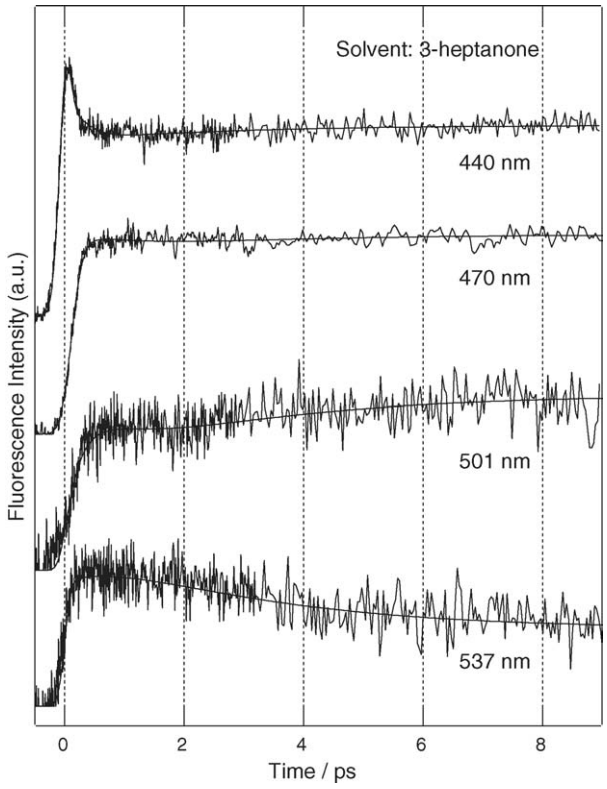

Fig. 3. Fluorescence time profiles measured with a femtosecond fluorescence up-conversion method for perylene in 3-heptanone.

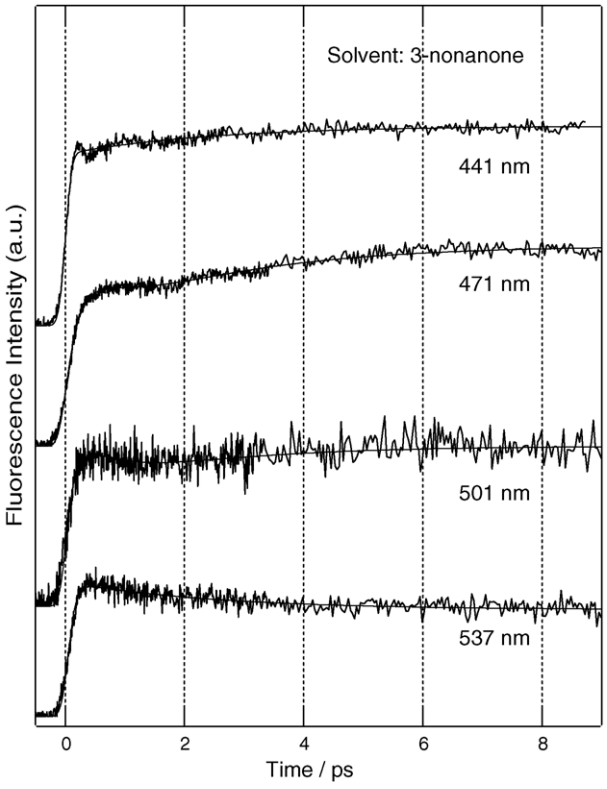

Fig. 5. Fluorescence time profiles measured with a femtosecond fluorescence up-conversion method for perylene in 3-nonanone.

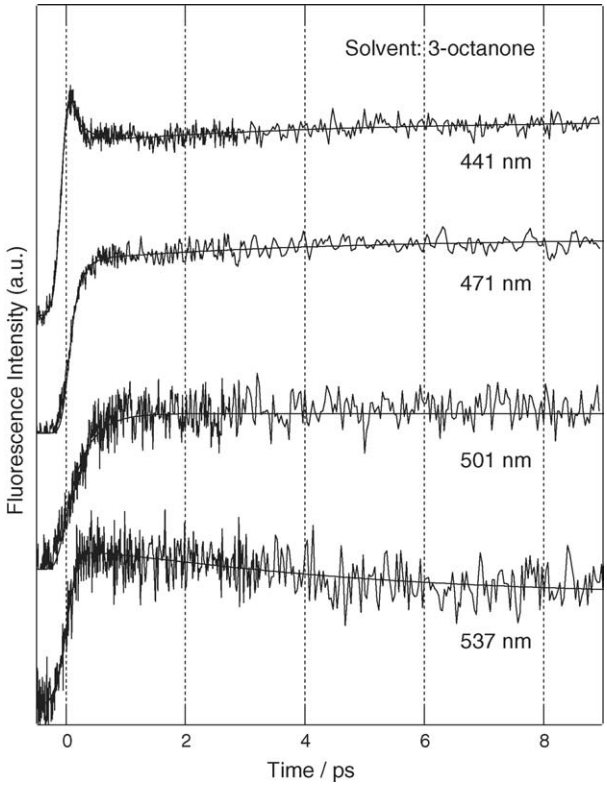

Fig. 4. Fluorescence time profiles measured with a femtosecond fluorescence up-conversion method for perylene in 3-octanone.

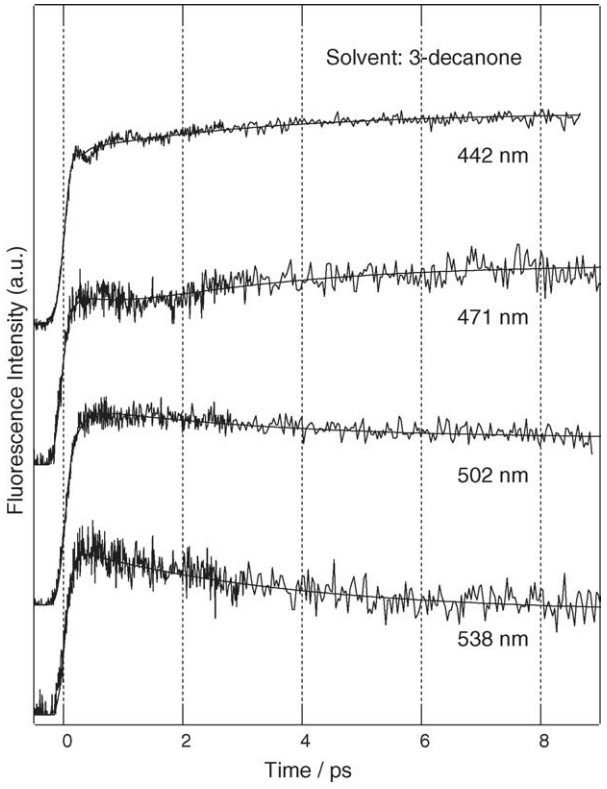

Fig. 6. Fluorescence time profiles measured with a femtosecond fluorescence up-conversion method for perylene in 3-decanone.

Fluorescence transients were individually fitted to a sum of four exponential functions by using an iterative deconvolution method. All fluorescence transients could be fitted by using following four components: 70–330 fs (τ_1), 0.6–1.1 ps (τ_2), 1.8–4.9 ps (τ_3), and a time constant of 4 ns, which corresponds to the S_1 lifetime of perylene. The early time behavior of the 0–0 transition is less clear-cut, because the 0–0 fluorescence profile at ca. 441 nm was disturbed by C–H Raman band of the solvent, which is more apparent in shorter chain-length solvent. Though a Raman component which assumed as 200 fs FWHM Gaussian function was involved for the analysis of 0–0 fluorescence profiles, an ultrafast decay component τ_1 was necessary for the best fit in 3-pentanone, 3-heptanone and 3-octanone. The τ_1 values of 0–0 transition are ambiguous because its values vary depending on the amplitude of Raman component, although the ultrafast decay component exists undoubtedly for these solvents. An ultrafast rise component τ_1 was necessary for the best fit in the deconvolution analysis of fluorescence profiles monitored at 0–1, 0–2 and 0–3 transitions. The τ_2 and τ_3 values obtained from individual fit are common in the same solvent and independent of observed transition. Therefore, the τ_2 and τ_3 values were re-evaluated with global analysis for each solvent, and the results agreed with those obtained from individual fit within the uncertainties.

The lifetimes and amplitudes of fluorescence profiles at each transition in each solvents are summarized in Table 1. The ultrafast rise component τ_1 was observed in all the wavelength range except 0–0 transition. An ultrafast decay component was observed for the fluorescence transient measured at 0–0 transition, but its value is not clear because of disturbance from solvent Raman band. We couldn't conclude the ultrafast decay at 0–0 transition corresponds to the ultrafast rise for the other transitions. Morandeira et al. have also found the ultrafast rise component (100–300 fs) for fluorescence profiles of perylene in toluene, however, these author avoided elaborate discussion because of complicated characteristics [24]. Their observation in sub picoseconds region agrees with our experimental data.

Fig. 7 shows solvent chain-length dependences of the lifetime for the medium component (τ_2) and for the slowest component (τ_3). As shown in Fig. 7, τ_2 does not change significantly in the solvents we used, thus, it can be attributed to the relaxation having pure IVR character. On the other hand, τ_3 exhibits noticeable solvent dependence. Therefore, τ_3 can be assigned to VET or SA-IVR. Blanchard et al. reported an analysis of VER of ground-state (S_0) perylene in several ketone solvents by using picosecond stimulated emission spectroscopy, and found that the VET rates were in 10–50 ps range [9]. This time constant is much longer than the τ_3 value observed in the present study, 1.8–4.9 ps, even taking the difference in the electronic states, S_0 and S_1, into account. It is also noted that Schwarzer et al. reported the intramolecular energy transfer rate of 1.2–4 ps and the VET rate of 21 ps for electronically excited linked azulene-aryl compounds [25]. This suggests also that τ_3 should be due to SA-IVR rather than VET to solvents. The time constant τ_3 is also very close to the picoseconds IVR rate that we have found in S_1 perylene in MTHF [12,13]. In a few picoseconds time region, the transient vibrational temperature is still higher than the statistical-limit temperature obtained by assuming that vibrational energy is equi-partitioned over all the vibrational modes of solute [13]. Therefore, there is a possibility that τ_3 reflects the SA-IVR process rather than VET.

Table 1
Lifetimes and relative amplitudes of fluorescence time profiles for five ketone solvents[a]

Solvent	Observed transition	τ_1 (ps)	A_1	τ_2 (ps)	A_2	τ_3 (ps)	A_3	τ_4 (ps)	A_4
3-Pentanone	0–0	0.1[b]	0.2				−0.1		0.8
	0–1	0.20	−0.6	0.93	0.3	1.95	−0.3	4000	0.7
	0–2	0.17	−0.8		0.3		−0.1		0.7
	0–3				−0.4		0.6		0.4
3-Heptanone	0–0	0.3[b]	0.2				−0.1		0.8
	0–1	0.14	−0.2	0.97	0.1	2.77	−0.1	4000	0.9
	0–2	0.27	−0.6		0.3		−0.3		0.7
		0–3			−0.3		0.6		0.4
3-Octanone	0–0	0.2[b]	0.2				−0.1		0.8
	0–1	0.14	−0.4	1.01	0.05	4.34	−0.15	4000	0.95
	0–2	0.33	−0.7		0.1		−0.1		0.9
	0–3				−0.1		0.4		0.6
3-Nonanone	0–0						−0.15		1.0
	0–1	0.23	−0.7	0.59	0.3	2.44	−0.3	4000	0.7
	0–2	0.21	−0.4		0.3		−0.2		0.7
	0–3	0.070	−0.4		0.2		0.8		
3-Decanone	0–0						−0.2		1.0
	0–1	0.12	−0.4	0.61	0.2	3.30	−0.25	4000	0.8
	0–2	0.17	−0.4		0.2		0.8		
	0–3	0.070	−0.6		0.4		0.6		

[a] $\tau_{1–4}$ and $A_{1–4}$ are lifetimes and relative amplitudes obtained from the global analysis of fluorescence time profile. A negative amplitude indicates a rise component.
[b] Lifetimes contains uncertainty disturbed by Raman scattering of the solvent.

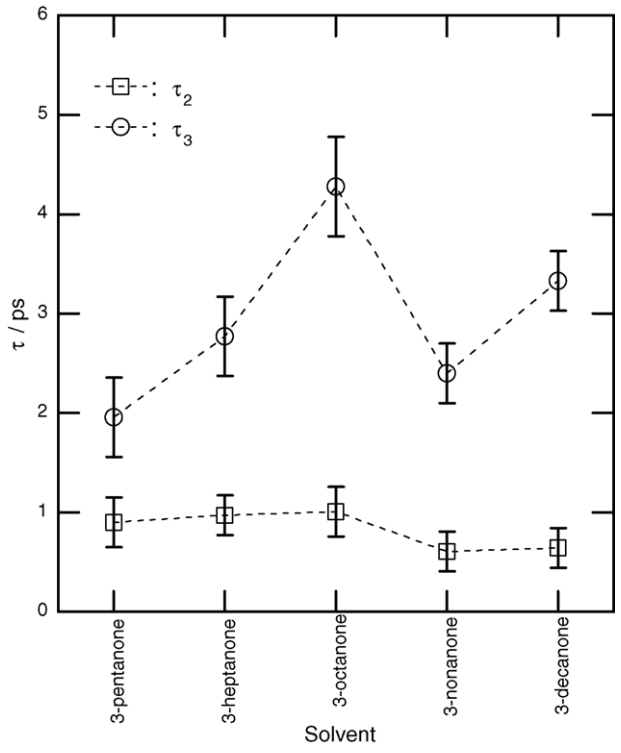

Fig. 7. Solvent chain-length dependence of the lifetime for the slow IVR component (τ_3, open circles) and the medium component (τ_2, open squares) of perylene.

The mechanism of SA-IVR is usually explained by the vibrational resonant anharmonic couplings between solute and solvents [2,6]. This is marked contrast to the conventional VET mechanism where V–T (vibration–translation) or V–L (vibration–libration) interactions play a dominant role. In SA-IVR, the vibrational excess energy which is deposited on the Franck–Condon active state(s) flows into the dark states within the solute molecule with assistance of solvents. We assume that such elastic interaction is the V–V (vibration–vibration) resonance coupling between solute and solvents.

As an increase of the solvent chain-length, the τ_3 value increases in the region both C_5–C_8, and C_9–C_{10}, while decreases suddenly between C_8 and C_9. On the other hand, the τ_2 value is constant for the C_5–C_8 and the C_9–C_{10} regions, but drops off slightly between C_8 and C_9. This sudden drop-off of decay rates, which is common for τ_2 and τ_3 processes, may be attributed to the change in structure of solvation cavity surrounding perylene. Goldie and Blanchard measured reorientation dynamics of perylene in ketone solvents, and reported that the reorientation of perylene can be expressed by a single exponential decay function for the C_5–C_8 ketone solvents while by a double exponential decay for the C_9 ketone solvent [9]. These results indicate that the structure of solvation cavity surrounding perylene changes from prolate for the C_5–C_8 ketones to oblate for the C_9 ketone [9,26]. Note that the change in cavity structure even affects the pure IVR rates as well as the SA-IVR rates as indicated in Fig. 7.

By the way, how can we explain the moderate increase in τ_3 for the C_5–C_8 and the C_9–C_{10} regions, where the cavity structure is considered to be the same? Solute–solvent interactions are classified into three categories: V–V, V–T and V–L interactions as mentioned above. The V–T interaction is a key factor for simple solvents with small internal degrees of freedom [20]. The V–T and the V–L interactions also play important roles for flexible solute molecules such as triphenylmethane dyes [27]. On the other hand, the V–V interactions are considered to be very important for solvents with large internal degrees of freedom as demonstrated by the semi-empirical model calculations by Kable and Knight [20]. As for the perylene–ketone system, the V–V interaction is expected to be a main factor in SA-IVR since ketone solvents have a large internal degree of freedom. When SA-IVR is assumed to be originated from anharmonic couplings between solute and solvent molecules in the first solvation shell, the rate can be obtained in the form of the Golden rule, in which the total rate constant k is given by:

$$k = \frac{2\pi}{\hbar^2}|V|^2\rho \tag{1}$$

where V is the matrix element between molecular levels and ρ is the total vibrational density of bath states, which include both solute and solvent vibrational modes. The total vibrational density of bath states, ρ may be given by:

$$\rho = \rho_M + N(\rho_S + \rho_{MS}) \tag{2}$$

where ρ_M is the vibrational density of the solute states, N the number of the solvent molecules in the first solvation shell, ρ_S the vibrational density of the solvent states, and ρ_{MS} that of solute–solvent combination states.

By counting possible combinations of normal vibrational modes for solute and solvents, ρ_M, ρ_S and ρ_{MS} can be estimated. The normal vibrational modes were computed by WinMOPAC version 3.0 (Fujitsu). Because FWHM of the excitation pulse was ca. 80 fs, the energy uncertainty width of the final-state manifold is estimated to be ca. 420 cm^{-1}. Therefore, ρ_M, ρ_S and ρ_{MS} were counted in an energy interval $\pm 210\,cm^{-1}$ with respect to difference in quantum number of initially excited state. Note that only one solvent molecule was taken into account in this calculation. Thus, the number of solvent molecule, N, in the first solvation shell, which interact strongly with solute molecule should be multiplied by the result in order to reproduce τ_3. We estimated the number of the solvent molecules in the first shell, N, by Eqs. (1) and (2), using experimental values of the VER rates, τ_3, and calculated density of vibrational bath states. The vibrational density of states for a pair of solute and solvent, $\rho_M + \rho_S + \rho_{MS}$, and the estimated number of solvent molecules, N, for each solvents are presented in Table 2. The estimated N becomes abruptly smaller as the chain-length increases for the C_5–C_8 and the C_9–C_{10} regions. It is also noted that the IVR rate is proportional to the overall density of bath states, ρ according to Eq. (1). However, our experimental finding is opposite; the lower ρ is, the faster the SA-IVR rate becomes.

To explain this result, we assume that the only low-order couplings with the low-quantum vibrational states of the bath may contribute to enhance SA-IVR (Fig. 8). As a background of this model, recent experimental studies on IVR in solution indicated the IVR rates are well explained by such a hierarchical or tier model [1,14–18]. In the tier model, the initial vibrational

Table 2
The observed IVR rates and the calculated vibrational densities of bath for total and low-order couplings ($l = 2, 3$), and the number of the solvent molecule in the first solvation shell, which are estimated by Eqs. (1)–(5)

Solvent	τ_3 (ps)	$\rho_M + \rho_S + \rho_{MS}$ (cm)	N	$(\rho_M + \rho_S + \rho_{MS})_{l=2,3}$ (cm)	$N_{l=2,3}$
3-Pentanone	2.0	264	0.15	1.10	3.4
3-Heptanone	2.8	10780	0.046	1.60	1.5
3-Octanone	4.3	59350	0.0094	1.85	0.82
3-Nonanone	2.4	309600	0.038	2.11	1.3
3-Decanone	3.3	2429000	0.015	2.33	0.80

energy is not distributed over all the vibrational modes simultaneously, but flows through specific low-order couplings step by step. Thus, it is naturally expected that the IVR rates are governed not by the total density of vibrational states, but by the partial density of states responsible for specific low-order couplings. For the case of SA-IVR, there would also be a possibility that specific couplings between the initially excited state and the energetically nearby bath states determine the SA-IVR rates. These nearly resonant vibrational states of solvents couple with solute vibrational states through an elastic interaction and enhance SA-IVR. Thus, when the number of strongly coupled states remains constant or decreases as solvent chain becomes longer, our experimental result of the SA-IVR rates will be explained.

To investigate this possibility, we analyzed the number of one- and two-phonon resonant couplings for each solvent by a direct counting method. For every combination between initial and final (bath) states, the difference of vibrational quantum number, l, is defined as:

$$l = \sum_{k \in \text{all modes}} \left| \nu_k^{\text{i}} - \nu_k^{\text{f}} \right| = |\Delta\nu_i| + \sum_{k \neq i} \nu_k^{\text{f}} \tag{3}$$

where ν_k^{i} is the vibrational quantum number of kth vibrational mode for the initial state, ν_k^{f} is that for the final state, and $\Delta\nu_i$ is a change in quantum number of initially excited vibrational mode. From the previous report [10], the VER in S_1 perylene excited at $\nu' = 2$ occurs not only via a successive route, $|2\rangle \rightarrow |1\rangle$ followed by $|1\rangle \rightarrow |0\rangle$, but also via a direct route, $|2\rangle \rightarrow |0\rangle$. The VER time constants of perylene in MTHF solution were obtained as 2.7 ps for $|2\rangle \rightarrow |1\rangle$, 1.8 ps for $|1\rangle \rightarrow |0\rangle$, and 700 fs for $|2\rangle \rightarrow |0\rangle$. We assume that the lifetime, τ_3, found in the present study reflects the picosecond successive process, therefore, $\Delta\nu_i = 1$ for our case. The vibrational coupling matrix element is approximated by:

$$V = \langle V(l) \rangle = V_0 \alpha^{l-2} \tag{4}$$

The smaller $\Delta\nu$ is, the larger the matrix element becomes [28]. The rate constant is given by:

$$k = \sum_b R_{ab} \cong \frac{2\pi}{\hbar} \sum_{l \geq 2} V_0^2 \alpha^{2(l-2)} \rho(l) \tag{5}$$

V_0 and α have been determined as $V_0 = 0.59\,\text{cm}^{-1}$ and $0.46 < \alpha < 0.5$ for perylene in MTHF solution [13]. We estimated the number of the solvent molecules, $N_{l=2,3}$, by Eqs. (1)–(5), using experimental VER rates and calculated density of low-order coupled bath states, $\rho_{l=2,3}$. Calculated vibrational densities and the number of the solvent molecules in the first shell are summarized in Table 2.

When all vibrational modes of bath states interacting with a solute molecule were considered, N became absurd as mentioned previously. Thus, we cannot explain the solvent-length dependence of the experimental SA-IVR rates by this model. However, when only the low-order couplings were taken into account, the vibrational density of bath states changed moderately, and the calculated numbers of solvent molecule, $N_{l=2,3}$, are in the reasonable range. Hence, we can explain the solvent-length dependence of experimental IVR rates from this calculation at least qualitatively on the basis of the tier V–V coupling model. The τ_3 behavior would be also explained by the solvent viscosity, which is usually employed to explain the solvent chain-length dependence by the V–T coupling mechanism. Further study is required to conclude which process (V–V or V–T) is dominant.

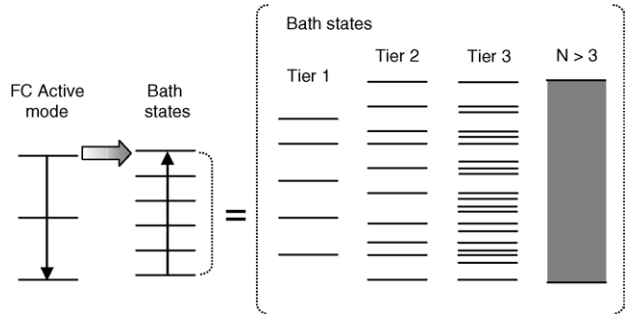

Fig. 8. Schematic representation of the SA-IVR mechanism where the only specific low-order couplings with bath states govern the IVR rate. The initial vibrational energy is not distributed over all the vibrational modes simultaneously, but flows through specific low-order couplings step by step. Bath states include the intramolecular vibrational states of solute which is not initially excited, the vibrational states of solvent molecules within a first solvation shell, and the solute–solvent combination states.

4. Conclusions

We have investigated VER of S_1 perylene in several ketone solvents with an excess vibrational energy of ca. $2800\,\text{cm}^{-1}$ ($\nu' = 2$ level of ring-breathing mode, ν_7) by femtosecond time-resolved fluorescence measurements. The temporal evolution of fluorescence time profiles occurs on the following distinct timescales: 70–330 fs (τ_1), 0.6–1.1 ps (τ_2), 1.8–4.9 ps (τ_3). The medium component τ_2 may be attributed to the pure IVR, since it does not change significantly in the solvent we used. On the other hand, the slowest component τ_3 exhibited noticeable solvent dependence. The drastic change of decay rates between C_8 and C_9, which is common for τ_1, τ_2 and τ_3 processes, may be attributed to the change in a cavity structure surrounding perylene. In SA-IVR, intramolecular vibrational couplings are affected by elastic or quasi–elastic interactions between solute and solvents. It was shown that τ_3 behavior within the same solvent structure can be explained qualitatively by the tier V–V coupling mechanism.

Acknowledgements

The present work is supported by a Grant-in-Aids for Scientific Research (No. 17350001 and No. 16550114) from the Ministry of Education, Science, Sports, and Culture of Japan.

References

[1] J. Assmann, M. Kling, B. Abel, Angew. Chem. Int. Ed. 42 (2003) 2226.
[2] J.C. Owrutsky, D. Raftery, R.M. Hochstrasser, Annu. Rev. Phys. Chem. 45 (1994) 519.
[3] S. Sato, T. Kitagawa, Appl. Phys. B 59 (1994) 415.
[4] Y. Mizutani, T. Kitagawa, Bull. Chem. Soc. Jpn. 75 (2002) 965.
[5] T. Nakabayashi, H. Okamoto, M. Tasumi, J. Phys. Chem. A 102 (1998) 9686.
[6] J.S. Baskin, H.-Z. Yu, A.H. Zewail, J. Phys. Chem. A 106 (2002) 9837.
[7] R. von Benten, O. Link, B. Abel, D. Schwarzer, J. Phys. Chem. A 108 (2004) 363.
[8] R. von Benten, A. Charvat, O. Link, B. Abel, D. Schwarzer, Chem. Phys. Lett. 386 (2004) 325.
[9] S.N. Goldie, G.J. Blanchard, J. Phys. Chem. A 105 (2001) 6785.
[10] S.N. Goldie, G.J. Blanchard, J. Phys. Chem. A 103 (1999) 999.
[11] Y. Jiang, G.J. Blanchard, J. Phys. Chem. 98 (1994) 9411.
[12] T. Kasajima, S. Akimoto, S. Sato, I. Yamazaki, Chem. Phys. Lett. 375 (2003) 227.
[13] T. Kasajima, S. Akimoto, S. Sato, I. Yamazaki, J. Phys. Chem. A 108 (2004) 3268.
[14] J. Assmann, R. von Benten, A. Charvat, B. Abel, J. Phys. Chem. A 107 (2003) 5291.
[15] J. Assmann, R. von Benten, A. Charvat, B. Abel, J. Phys. Chem. A 107 (2003) 1904.
[16] J. Assmann, A. Charvat, D. Schwarzer, C. Kappel, K. Luther, B. Abel, J. Phys. Chem. A 106 (2002) 5197.
[17] C.G. Elles, M.J. Cox, F.F. Crim, J. Chem. Phys. 120 (2004) 6937.
[18] C.G. Elles, D. Bingemann, M.M. Heckscher, F.F. Crim, J. Chem. Phys. 118 (2003) 5587.
[19] K. Sekiguchi, A. Shimojima, O. Kajimoto, Chem. Phys. Lett. 370 (2003) 303.
[20] S.H. Kable, A.E. Knight, J. Phys. Chem. A 107 (2003) 10813.
[21] H.J. Bakker, J. Chem. Phys. 98 (1993) 8496.
[22] V.M. Kenkre, A. Tokmakoff, M.D. Fayer, J. Chem. Phys. 101 (1994) 10618.
[23] S. Akimoto, I. Yamazaki, T. Sakata, M. Mimuro, J. Phys. Chem. A 106 (2002) 2237.
[24] A. Morandeira, A. Fürstenberg, J.-C. Gumy, E. Vauthey, J. Phys. Chem. A 107 (2003) 5375.
[25] D. Schwarzer, C. Hanisch, P. Kutne, J. Troe, J. Phys. Chem. A 106 (2002) 8019.
[26] Y. Jiang, G.J. Blanchard, J. Phys. Chem. 98 (1995) 6436.
[27] Y. Nagasawa, Y. Ando, D. Kataoka, H. Matsuda, H. Miyasaka, T. Okada, J. Phys. Chem. A 106 (2002) 2024.
[28] B. Fourmann, C. Jouvet, A. Tramer, J.M. Le Bars, Ph. Millie, Chem. Phys. 92 (1985) 25.